Hindawi
Advances in Civil Engineering
Volume 2024, Article ID 9922218, 13 pages
https://doi.org/10.1155/2024/9922218

Research Article

Influence and the Control of Shield Tunneling on Ancient Tower Vibration

Xu Liang,[1] Jian Xu,[1] Yapeng Zhang,[2] Xinquan Gao,[3] Xuetao Zhou,[2] Zonghao Yuan,[3] Min Zhang,[4] Jian Wu,[5] and Long Liu[6]

[1]*Hangzhou Urban Infrastructure Construction Management Center, Hangzhou, China*
[2]*Power China Huadong Engineering Corporation Limited, Hangzhou 310005, China*
[3]*College of Civil Engineering, Zhejiang University of Technology, Hangzhou 310014, China*
[4]*Institute of Transportation Engineering, Zhejiang University, Hangzhou 310000, China*
[5]*Zhejiang Engineering Research Center of Green Mine Technology and Intelligent Equipment, Hangzhou 311100, China*
[6]*Zhejiang Huadong Engineering Construction and Management Corporation Limited, Hangzhou 310030, China*

Correspondence should be addressed to Zonghao Yuan; yuanzh@zjut.edu.cn

Received 27 October 2023; Revised 22 January 2024; Accepted 23 January 2024; Published 5 February 2024

Academic Editor: Chao Zou

In recent years, to effectively mitigate the issue of urban traffic congestion, tunnels have become widely used new type of road. However, when the soil layer is excavated and disturbed, the resulting vibration affects the safety of the buildings above it, especially for ancient buildings that are very sensitive to vibrations. Taking the White Tower in Hangzhou as an example, in this paper, the vibration response propagation of large-diameter shield tunnel excavation to adjacent ancient towers is studied through field measurements. The vibration response of the unexcavated south line tunnel is predicted by using 3D numerical analysis software, and the optimal construction parameters are obtained. The study found that the frequency domain component of the White Tower bedrock vibration caused by shield tunneling is mainly 5–20 Hz, and the vibration response attenuates significantly beyond 40 m. Further, reducing the propulsive force can reduce the vibration response of the White Tower; therefore, controlling the propulsion and reducing the tunneling velocity can reduce the vibration response.

1. Introduction

In recent years, with the acceleration of urbanization, urban traffic is becoming increasingly congested and land space is declining. Therefore, the development of underground space has become a potential solution to mitigate this problem. For the excavation of underground tunnels, the most common methods include open excavation, cover excavation and reverse construction, shotcrete anchor concealed excavation, and the tunnel boring machine (TBM) shield method. The shield method is widely used in modern tunnel construction because it can avoid the interference of weather, has little disturbance to the surrounding soil, and requires fewer construction workers.

Over the past several years, shield-tunneling technology has improved significantly, allowing the construction of tunnels with a large diameter, large buried depth, long distance, and complex strata. However, tunnel excavation has an increasing impact on the surrounding environment. Due to the aggravated geotechnical dynamic interaction caused by the shield cutter head, during the construction of large-diameter tunnels, the vibration response caused by the shield tunneling has a greater impact on nearby buildings.

In particular, the shield tunnel cannot avoid interactions with adjacent ancient buildings due to the route planning involved in the excavation process. Further, ancient buildings are very sensitive to the vibration from surrounding environments, and the excessive vibration during shield excavation may cause the cracking of the ancient building structure and the falling of fragments. Due to the "irrecoverability" of ancient buildings, cracking, even collapse caused by large vibrations, is irreversible; so, the protection of ancient buildings should be considered from the perspective of the safety and integrity of ancient buildings. The vibration

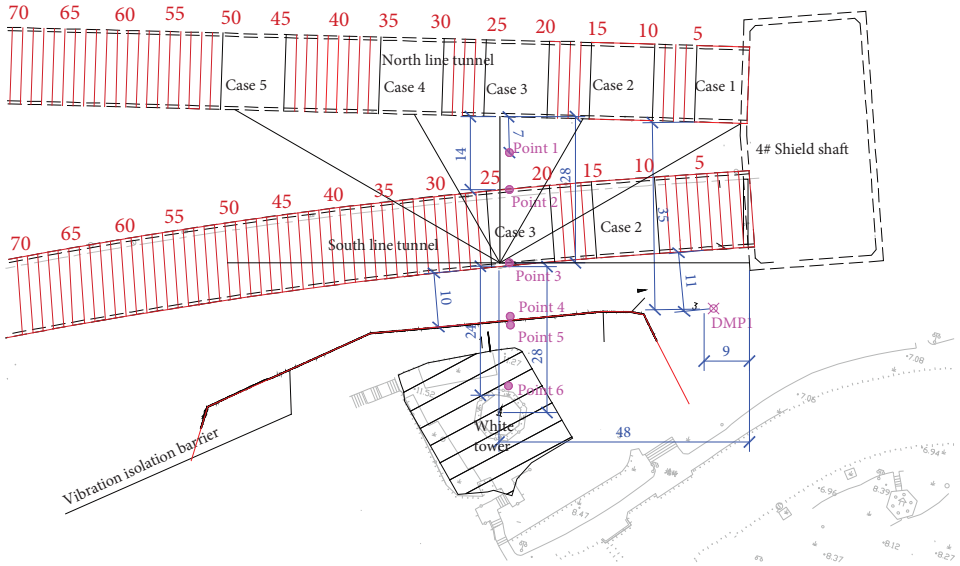

Figure 1: Location plan of measuring points.

protection of ancient buildings along the shield-tunnel excavation route is a crucial problem that should be solved.

The main vibration sources for buildings come from metro lines (including the tunneling and operation phase), piling, and road traffic. Fiala et al. [1] predicted the vibration and reradiated sound induced by ground traffic in buildings by studying the structural and acoustic responses of buildings to incident wavefields generated by high-velocity ground rail traffic. Similarly, Avci et al. [2] used finite element modeling to analyze and evaluate the vibration caused by trains on the ground of buildings. Kuo et al. [3] introduced a double-tunnel model, which improves the accuracy of vibration prediction for underground railways by calculating the interactions between the two tunnels. Wan et al. [4] monitored the vibration response of a subway tunnel in operation and proposed an identification method for structural modal parameters. Zou et al. [5] developed a computational model for train-generated vibration and studied the vibration transmission modes in transmission structures in architectural design. Gupta et al. [6] studied the influencing factors of underground vibration propagation through parameter analysis; their results show that the shear modulus of the soil mass will significantly affect the propagation of vibration waves. Zhang et al. [7] conducted model tests with a swept frequency load, proposed a new composite cross-passage, and studied its vibration-reduction effect. Zou et al. [8] measured the vibration and noise of subway trains during operation, put forward a prediction model of the vibration and noise of subway car depot, and verified it. Noori et al. [9] used a semianalytical model of the track–tunnel–ground system to calculate the energy flow generated when a train passed by, concluding that a dynamic vibration absorber would be an effective countermeasure to mitigate the ground vibration caused by the railway. Zou et al. [10] measured the train-induced vibrations and compared with limitation of FTA criteria, and concluded that the measured vertical vibrations were less than the FTA limit. He and Tao [11] used a coupled method of finite element analysis and on-site testing to predict

Table 1: Test equipment.

Number	Name	Model
1	Signal acquisition instrument	INV3062C
2	Engineering platform software	DASP-V11
3	Low-frequency acceleration–velocity sensor	941B
4	Downhole vibrometer	JX941

the impact of train operation on buildings. In terms of building vibration from piling, Chen et al. [12] established a numerical model to analyze the influence of different piling parameters on the vibration of adjacent tunnels, and obtained the limit value of the peak vibration of the tunnel caused by piling construction. Shiguang and Songye [13] studied the positioning of the pile driving vibration source by establishing a 3D finite element model of vibratory sheet pile driving, and verified the model through field tests. Rainer et al. [14] studied the interactions between vertically vibrating sheet piles and the surrounding ground using sensors on vibrators and on the ground near the sheet piles, concluding that the vibration frequency is an important parameter for installing sheet piles with high efficiency and in an environmental-friendly manner. Another important vibration source is road traffic, Li et al. [15] proposed a semianalytical and seminumerical method for predicting the ground vibration caused by traffic flow by establishing a vehicle–road–soil coupling model. Fang and Li [16] conducted field tests on the ground vibration caused by traffic loads and found that the vibration attenuation decreased rapidly within 10 m, and there was almost no vibration within 57 m.

In comparison to the abovementioned vibration sources, the vibration induced by the shield-tunneling process has a wider frequency band and a longer duration. Wu et al. [17] used a numerical model to study the TBM excavation process and concluded that the distance affected by vibration during hard rock tunnel construction is about 9 m, and the existence

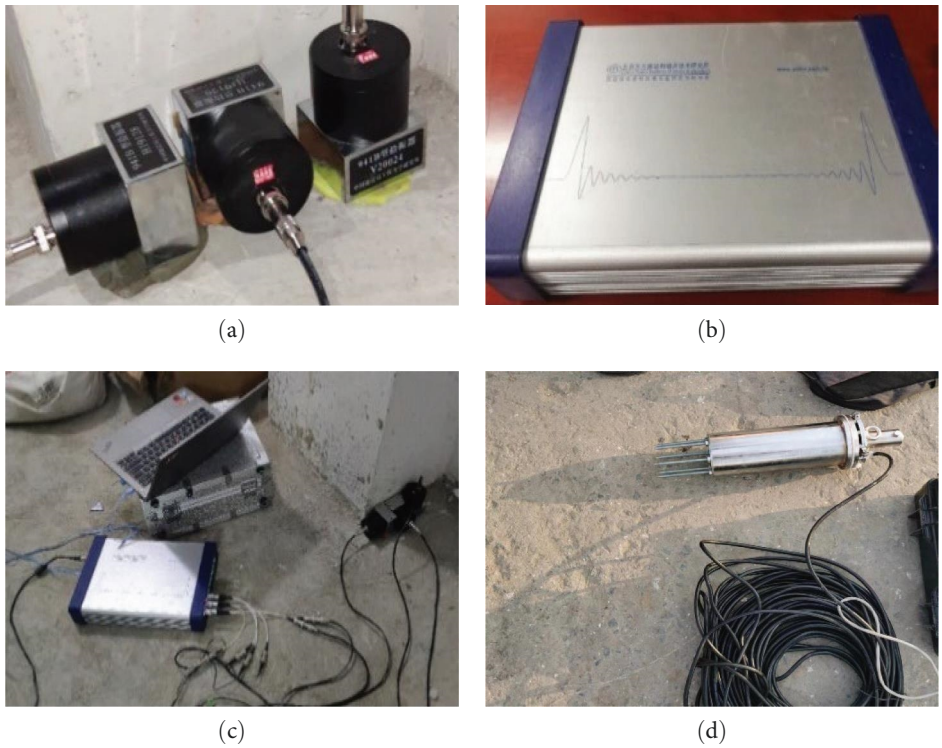

FIGURE 2: Test instrument: (a) low-frequency acceleration–velocity sensor; (b) signal acquisition instrument; (c) measured signal processing system; and (d) downhole vibrometer.

of ground buildings can suppress this vibration. Rallu et al. [18] performed vibration measurements inside a TBM, proposing an original methodology of signal processing to characterize the amplitude of the particle velocities, and also compared the vibration level with a threshold of disturbance to the local population. Liu et al. [19] developed a vibration-based prediction model using neural networks, which achieved both high prediction accuracy and feedback efficiency. Further, Lu et al. [20] studied the law of lateral and longitudinal vibrations in double-shield TBM construction, determining the vibration impact range of double-shield construction.

These related studies focus on the vibrations caused by underground train movement, piling, and road traffic, but do not study the impact of vibration caused by shield tunneling on surrounding buildings. In particular, when there are ancient buildings around shield-tunneling operations, the impacts of vibration are not clear; due to the sensitivity of ancient buildings to vibration responses and their irrecoverability in terms of damage, the requirements for vibration control are very stringent. To date, the impact of different conditions during shield-tunnel excavation on the vibration of adjacent shallow ancient buildings and their attenuation laws have not yet been clearly understood.

The goal of this research is to determine the interactions between the segment soil and the existing structure during tunnel excavation, which mainly focus on the influence of vibration on adjacent ancient buildings caused by tunneling. This study is based on the analysis of on-site measured data during the excavation of the northern tunnel; then, two unfavorable cases during the excavation of the southern tunnel were identified. The numerical inverse analysis method was used to predict the vibration response for these two unfavorable cases during the construction process of the southern tunnel. Furthermore, the relationship between construction parameters and vibration responses is explored.

2. Project Overview

2.1. Engineering Background. This vibration test is based on the water supply pipe corridor and road lifting project of Zhijiang Road in Hangzhou city, Zhejiang province (Fuxing Road and Zipu Road). The diameter of the shield is 15.03 m, which is a ultra-large-diameter shield. In this project, because there are many ancient buildings along the tunnel that cannot be avoided, it is necessary to carry out protective monitoring of the ancient buildings during construction and control the vibration response within a safe range. As seen in Figure 1, the White Tower is situated on the south side of the two tunnels. This White Tower has a history more than 1,000 years and is built on white stone. The height of the White Tower is up to 14.40 m, which is also the national cultural relic protection unit. The shield is divided into double-line tunneling, which is constructed in chronological order. The shield tunnel on the north line is 53 m away from the north side of the White Tower foundation and 24 m away from the north side of the White Tower foundation on the south line. The construction time of the north line tunnel is earlier than that of the south line tunnel. Therefore, the numerical model is verified using the data tested during the excavation of the north line tunnel, and the verified model is used to predict the vibration response

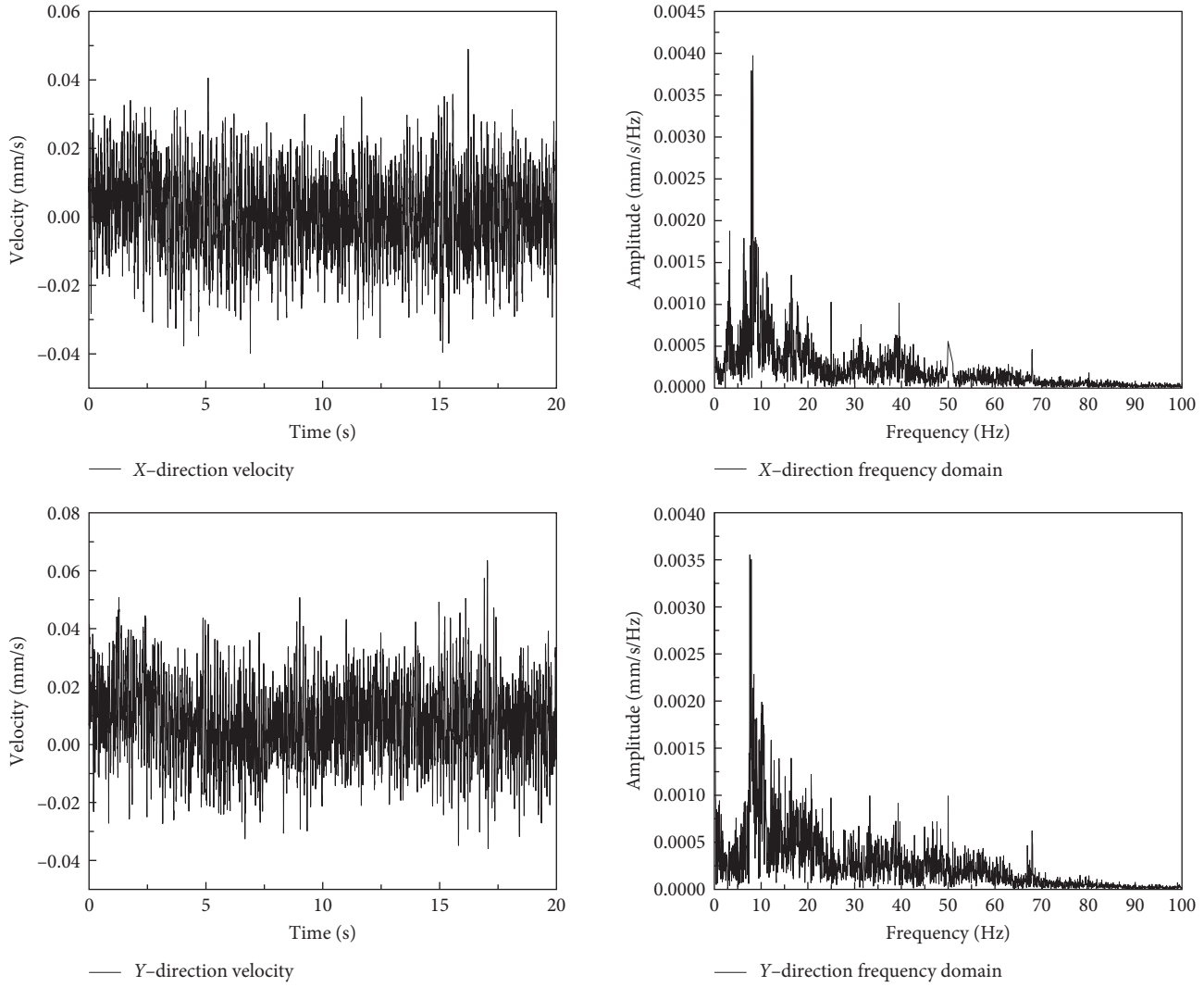

Figure 3: Time domain and frequency domain of case 3.

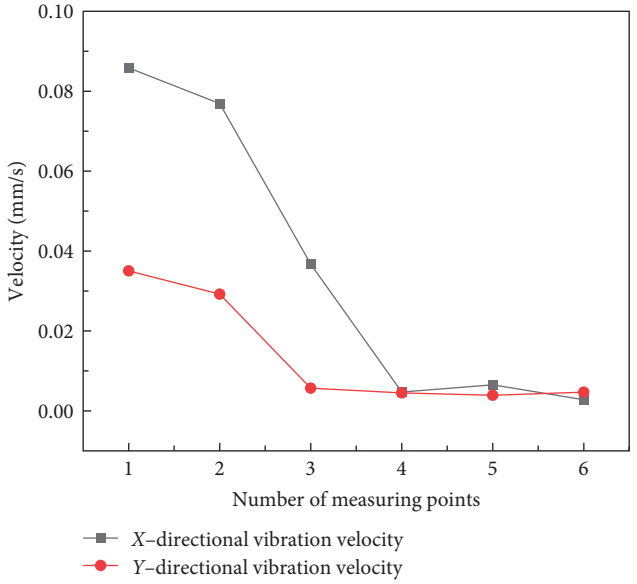

Figure 4: Vibration velocity of each measuring points for case 1.

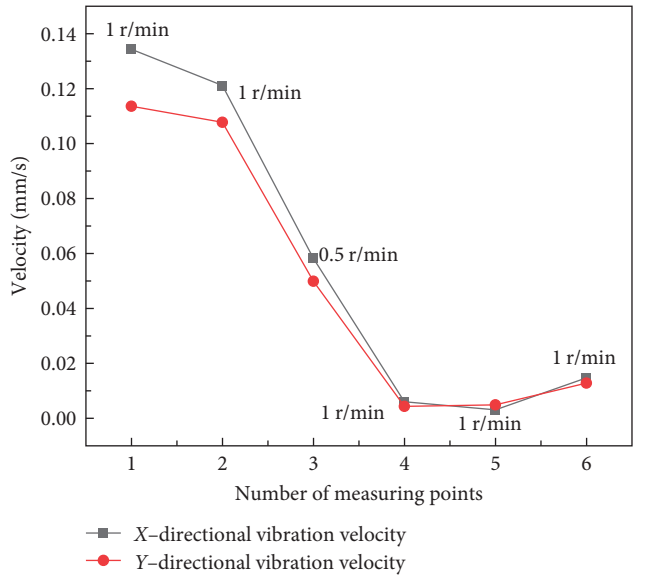

Figure 5: Vibration velocity of each measuring points for case 2.

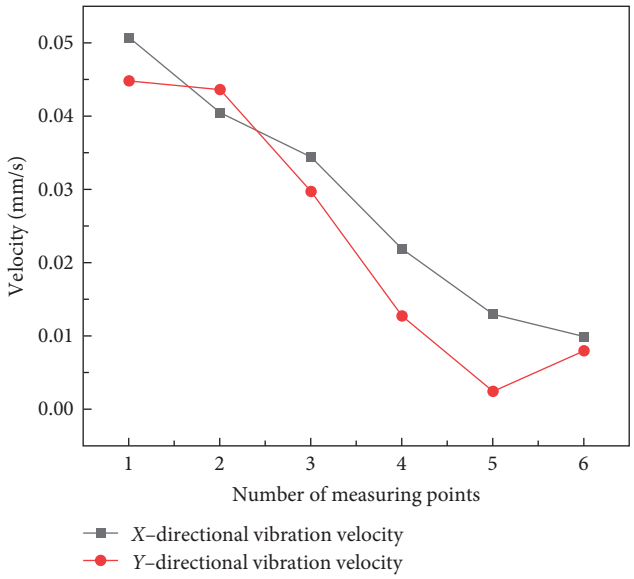

Figure 6: Vibration velocity of each measuring points for case 3.

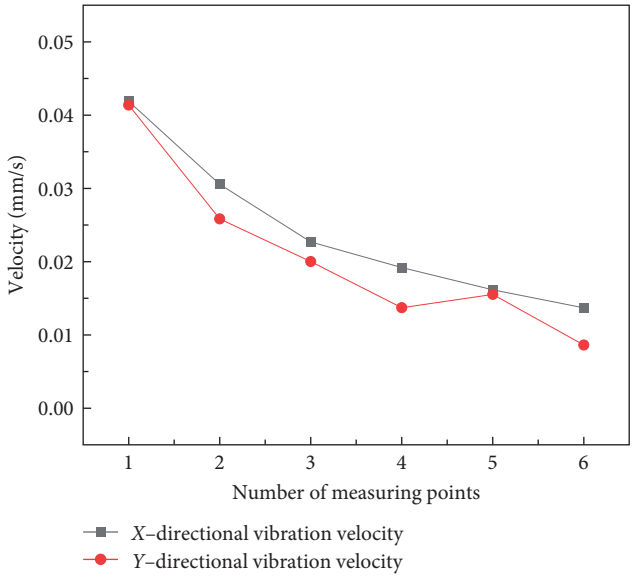

Figure 7: Vibration velocity of each measuring points for case 4.

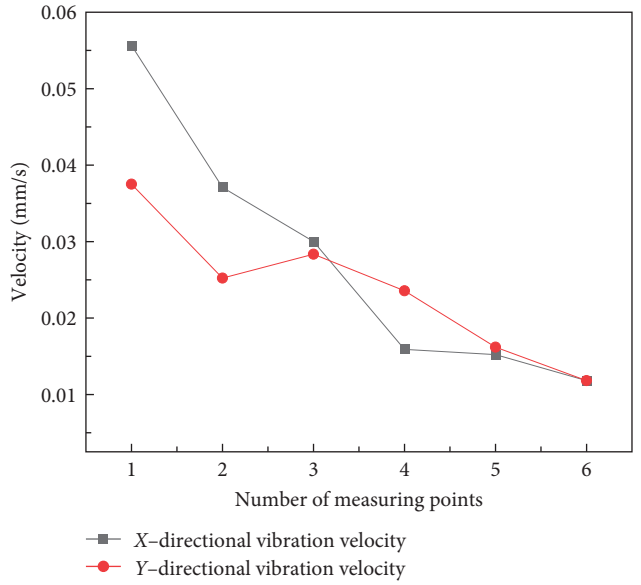

Figure 8: Vibration velocity of each measuring points for case 5.

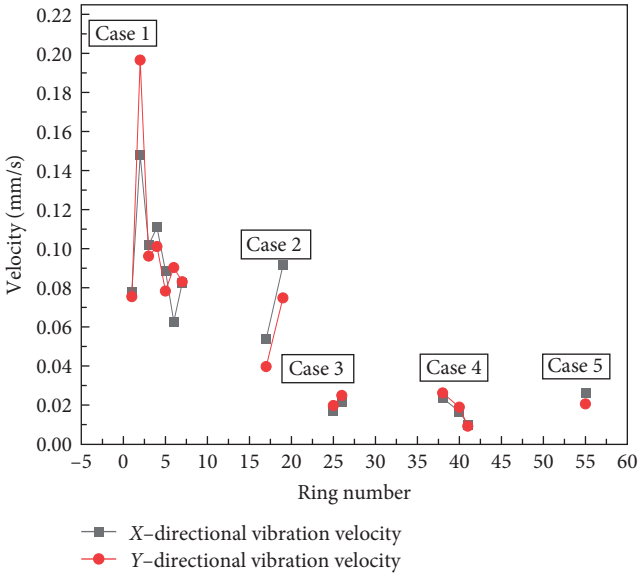

Figure 9: Attenuation law of the vibration velocity of DMP1 under different cases.

before the construction of the south line tunnel. Due to the low vibration limit of the White Tower, it is necessary to control the construction parameters prior to construction to reduce the impact.

2.2. Test Plan. As shown in Figure 1, five cross-sections were selected for this test, starting from the 4# shield tunnel in Fuxing Old Street, with the White Tower as the center. Cases 1–5 were set, with corresponding ring numbers ranging from 0 to 5, 10 to 15, 20 to 25, 30 to 35, and 45 to 50, respectively. The transverse survey line in the plant area is nearly perpendicular to the axis of the shield tunnel of the north line and arranged on the plane where the White Tower is located. The horizontal distance between the east–west direction and the 4# shield shaft is 48 m. Measuring points 1–6 are located 7, 14, 28.5, 38.5, 39.5, and 52.5 m (located on the foundation of the White Tower) south of the shield tunnel on the north line, respectively. Furthermore, a deep vibration measuring point (DMP1) is buried with a depth of approximately 5.5 m (around 11 m transverse distance from the south of the southern tunnel and 9 m away from the 4# shield shaft, Figure 1).

As shown in Table 1, the instruments tested mainly include the signal acquisition instrument, engineering platform software, four-port industrial 4G router, low-frequency acceleration–velocity sensor, and other equipment or tools: notebook computer, portable vibration calibrator, leveling instrument, angle iron, screw, magnetic suction seat, tape measure, tape marker, paint spraying, interphone, plasticine,

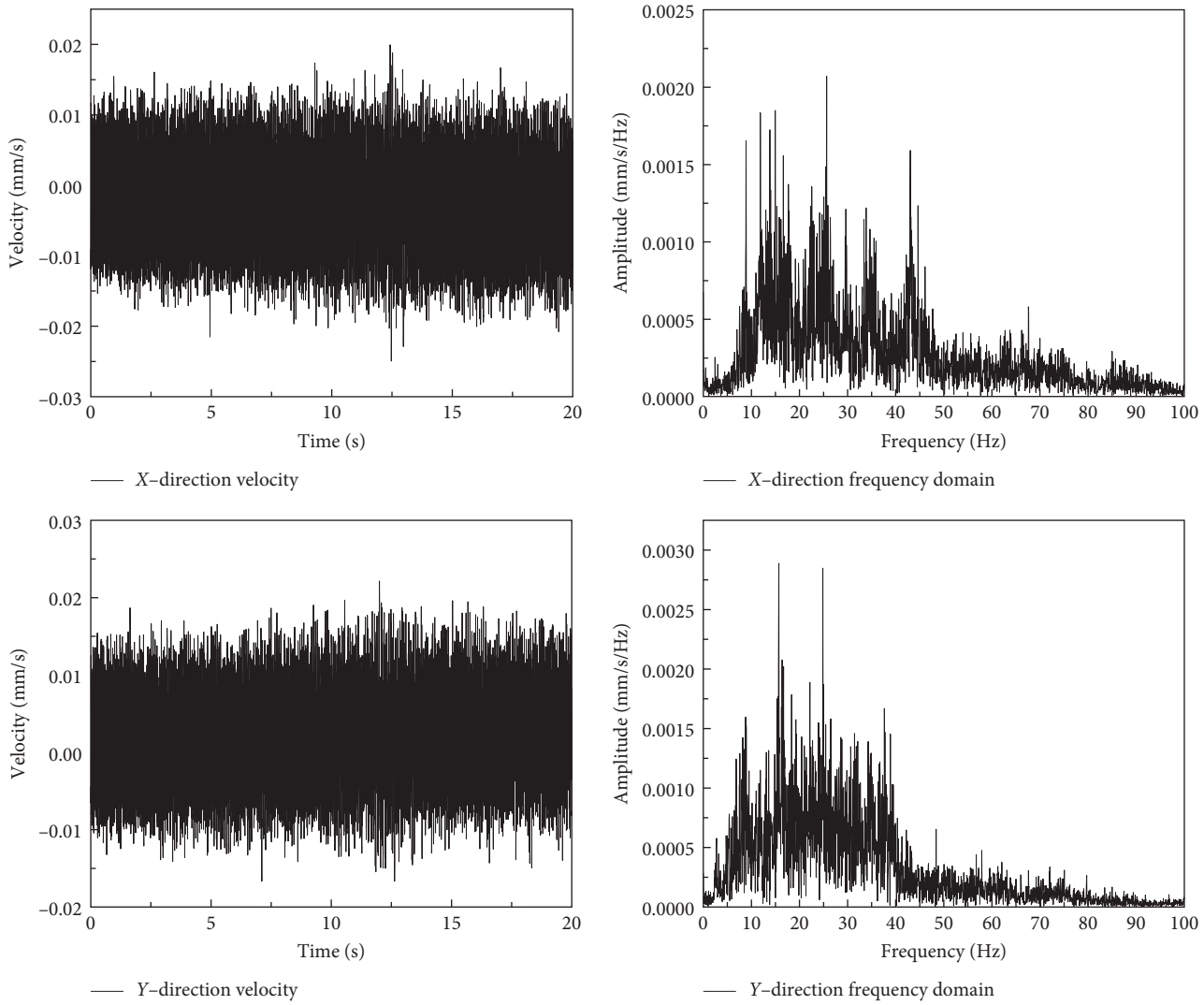

Figure 10: Time domain and frequency domain of DMP1.

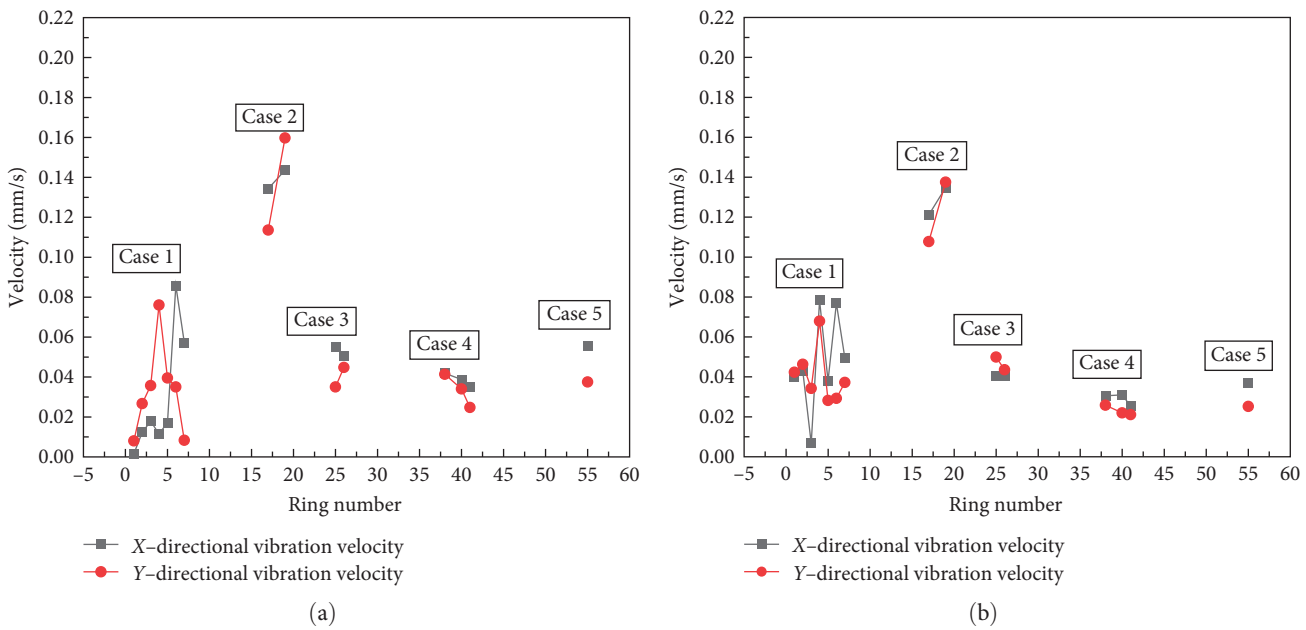

Figure 11: Attenuation law of vibration velocity under various cases: (a) measuring point 1 and (b) measuring point 2.

Table 2: Shield model material parameters.

Material	Thickness (m)	Density (kg/m^3)	Poisson's ratio	Elastic modulus (MPa)
Miscellaneous fill	1.5	1,930	0.35	140
Strongly weathered quartzite	1.1	2,070	0.22	1,130
Apoplectic quartzite	97.4	2,600	0.29	3,100
Square foundation	2	2,390	0.20	31,500
Base	1.5	2,200	0.20	30,000
Lining	0.6	2,500	0.20	38,000

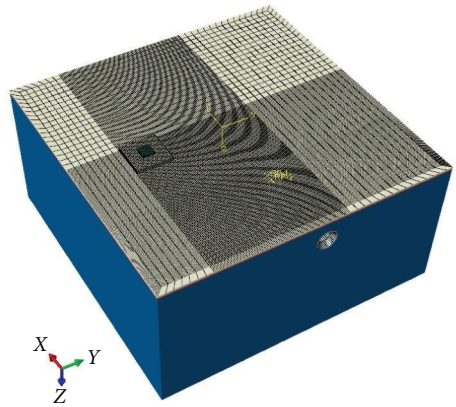

Figure 12: North line shield model.

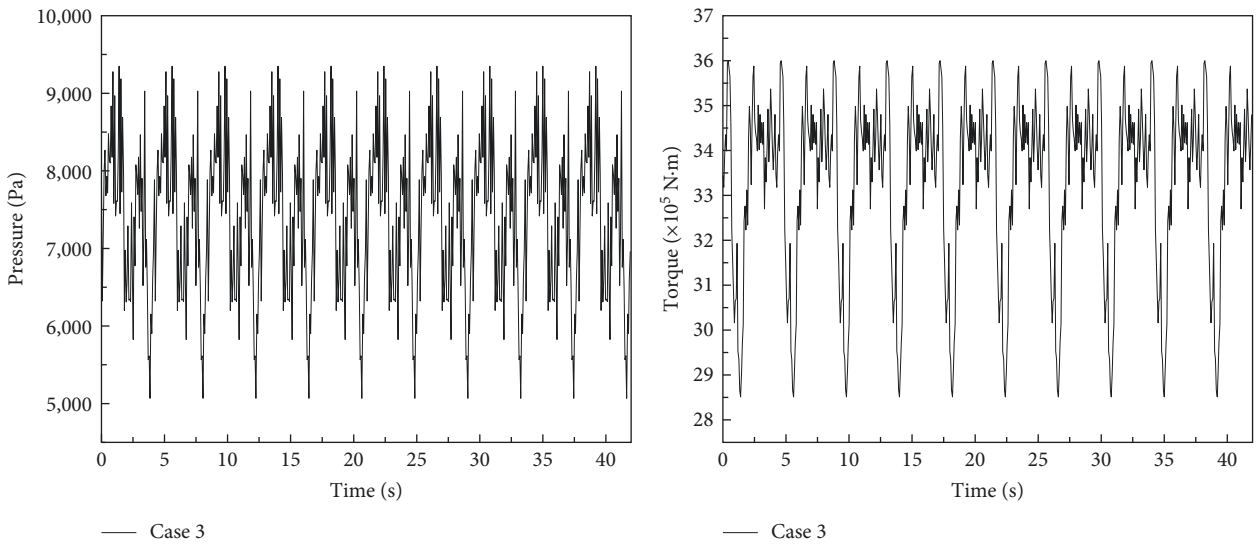

Figure 13: Model input pressure and torque under case 3.

epoxy resin AB glue, etc. The main test instruments are shown in Figure 2.

3. Test Results

3.1. Typical Testing Results in the Time and Frequency Domains. The *X*-direction is parallel to the shield-driving direction, and the *Y*-direction is perpendicular to the shield-driving direction. According to the field measurement results, the typical test results for measuring point 1 in case 3 are selected for time domain and frequency domain analysis. The time domain and frequency domain diagrams under case 3 are shown in Figure 3. From the time domain diagram analysis, it can be seen that the frequency band induced by excavation is wide, ranging from −0.04 to 0.04 mm/s. From the frequency domain diagram analysis, it can be seen that the main frequency domain of vibration is mainly distributed within 20 Hz.

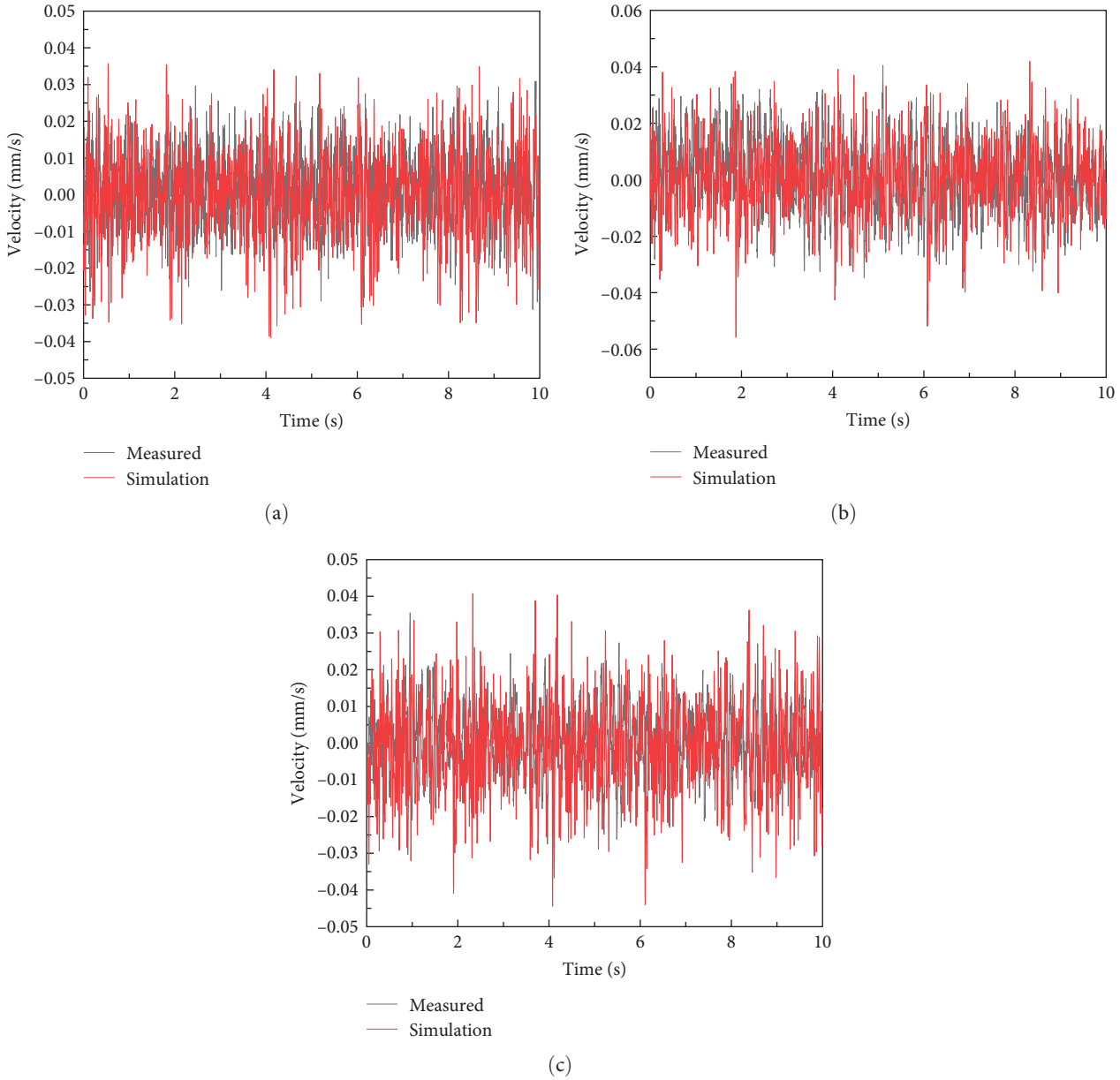

Figure 14: Comparison between simulation results and measured results under case 3: (a) measuring point 1; (b) measuring point 2; and (c) measuring point 3.

To investigate the vibration attenuation along the transverse direction, Figure 4 presents six designated measuring points. It can be seen that the vibration velocity gradually decreases from measuring point 1 to measuring point 6 in the lateral direction, with a more pronounced decline observed between point 1 and point 4. Specifically, the vibration velocity in the X-direction decreases from 0.08584 to 0.00471 mm/s, while in the Y-direction, it reduces from 0.03504 to 0.00499 mm/s. The rate of vibration attenuation is higher in the X-direction than in the Y-direction.

Moreover, it is evident that the amplitude reduction between point 4 and point 6 exhibits a relatively small reduction. Notably, once the lateral distance exceeds 40 m, the rate of vibration reduction diminishes. Furthermore, based on the analysis of case 1, it is apparent that transverse vibration attenuation is notable at a horizontal distance of 40 m from the vibration source.

A comparable test was conducted in case 2, as shown in Figure 5. In comparison to case 1, the vibration velocity increased due to the closer distance between the transverse measuring line and the head of the tunneling machine. Figure 5 reveals that the velocity of the shield cutter head at point 3 decreased from 1 to 0.5 r/min, accompanied by a reduction in its vibration peak value from 0.12 to 0.006 mm/s. The response of the measuring point after point 3, with a stable rotating velocity of 1 r/min, demonstrates relatively stable vibration levels, indicating no significant decreases, while the vibration response at point 6 increases, which is due to the

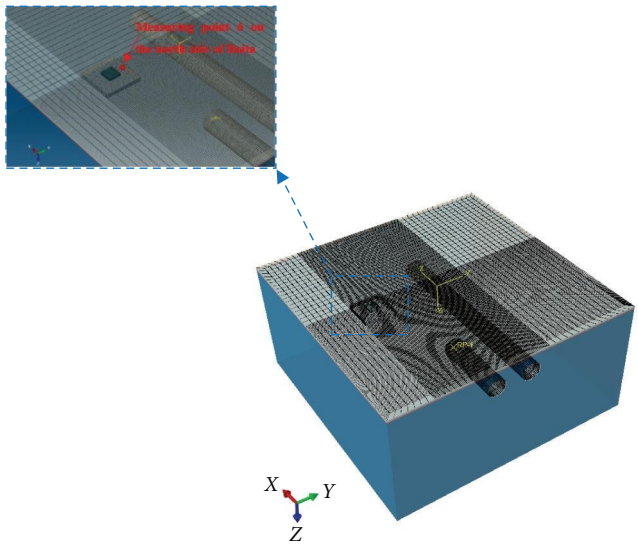

Figure 15: South line tunnel model and location of measuring point 6 on the north side of White Tower.

interference of construction during the test at this point. Hence, it can be concluded that the rotating velocity has a substantial impact on the vibration level during construction.

In case 3, both the cutter head and the White Tower are situated on the same cross-section. Figure 6 illustrates the measured data under case 3. Comparatively, the vibration levels of measuring points 1–5 in case 3 are lower than those of measuring points 1–5 in case 2 as shown in Figure 5. This discrepancy is due to the fact that, in case 3, the distance between the shield machine and the White Tower is minimized, and the construction parameters are intentionally reduced to ensure the safety of the White Tower.

In case 4, as shown in Figure 7, the vibration velocity at measuring point 1 is lower than that at measuring point 1 in case 3. It is evident that, in this case, the vibration velocity in the X-direction surpasses that in the Y-direction at each measuring point. As the shield moves away from the White Tower, the vibration velocity at each measuring point gradually decreases. Furthermore, the vibration velocity at each measuring point is lower than that when the cutter head of the shield is positioned on the right side of the White Tower (case 3).

In case 5, as shown in Figure 8, the shield machine has moved 50 m away from the protective ancient White Tower, prompting an increase in construction parameters such as thrust and torque. It is clear from the vibration velocity at point 1 that the velocity has increased; however, this increase is limited by the substantial attenuation of vibration propagation from the shield machine to the measuring point as it moves farther away from the vibration source. Even if the construction parameters are increased, their impact on the vibration velocity at this measuring point remains minimal.

The vibration response of DMP1, buried 39 m in front of the White Tower, for various cases is shown in Figure 9. It can be observed that the vibration of case 1 is the largest, and the peak value of the vibration response is 0.2 mm/s, which is obviously higher than that of case 1, where the position of the surface measuring point (measuring point 4) is close to that of DMP1, and the maximum peak vibration response 0.004 mm/s. This difference can be explained by the fact that the rock layer where DMP1 is present is below 5.5 m. When the vibration propagates in the rock, the attenuation is small. Therefore, the vibration response of DMP1 is higher than that of the point at the same position on the surface. Subsequently, the vibration response of DMP1 decreases gradually, and this trend can be attributed to the fact that, in case 1, DMP1 is closest to the vibration source.

Figure 10 shows the time domain and frequency domain of DMP1. It can be seen that the vibration bands inside the rock layer remains stable, which presents a steady-state vibration behavior. The vibration level is higher than that on the ground surface (located in the same vertical plane). Due to the closer distance between the buried point and the vibration source, it can be seen that the high-frequency vibration component is more obvious compared to that at the ground surface (Figure 3).

In the field tests, points 1–3—which are near the vibration source—exhibit the highest vibration levels in case 2, as shown in Figure 11. However, these points exhibit a consistent downward trend in subsequent cases. Second, during the shield tunneling of the north line, surface point 6 (near the White Tower bedrock) maintains a relatively low level of vibration response, while the vibration at deep measuring points generally decreases. Third, in case 4, the vibration velocity at points 1, 2, and 3 is lower than that in case 3. Furthermore, case 5, which is the final testing case conducted at a distance of 50 m from the measuring point, demonstrates an opposing attenuation pattern for points 1, 2, and 3 in comparison to case 4, resulting in an increase in the vibration velocity. This can be attributed to the shield being positioned 50 m away from the protective building, causing a significant increase in construction parameters. As a result, the vibration velocity at the measuring points in case 5 is slightly higher than that in case 4.

4. Simulation of Shield Tunneling

4.1. Model Establishment. According to the field drilling exploration results, the soil layer parameters of the shield tunneling model are shown in Table 2. The shield starts from the 4# working shaft, and the size of the finite element model is 200 m × 200 m × 100 m, including the White Tower foundation and 4# working shaft. The boundary size of the model infinite element is 5 m, and the grid is densified in the White Tower and shield area, as shown in Figure 12.

As shown in Figure 13, the pressure and torque input in the model are obtained from the actual construction sites, which can be extracted from the construction parameter recording. The simulation results of test point 6 after the simulation are compared with the field-measured results of test point 6 for northern line tunneling in case 3 (Figure 14). The simulation results are basically consistent with the measured vibration velocity band, and the peak vibration velocity is almost the same.

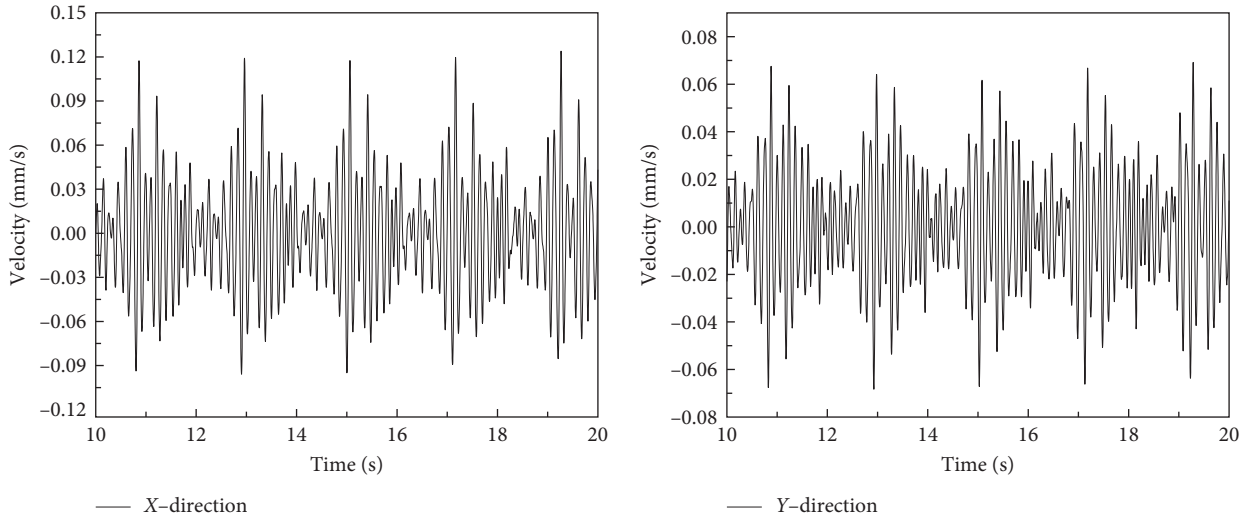

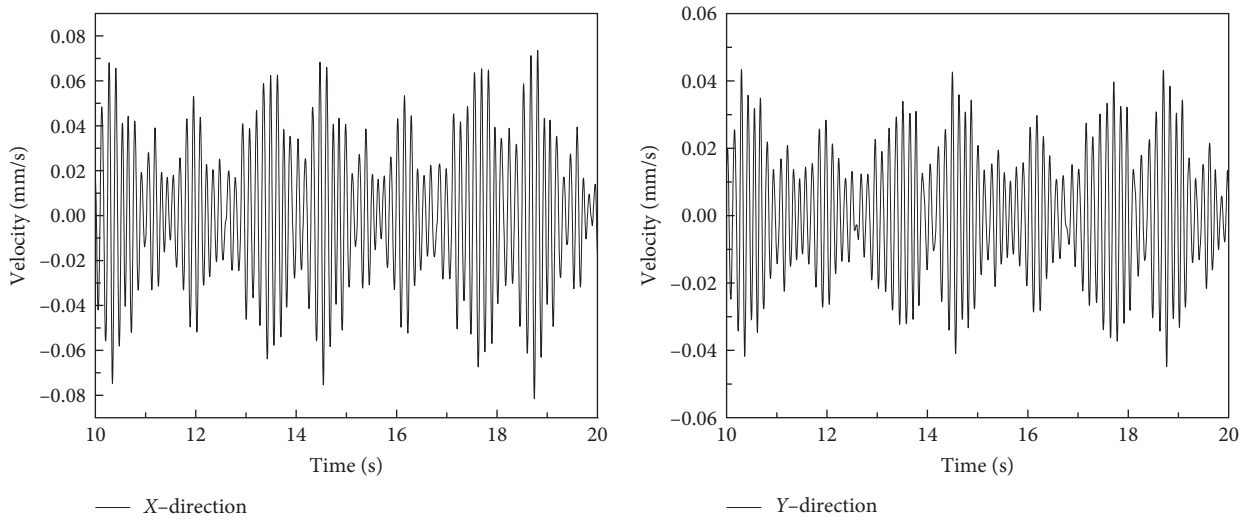

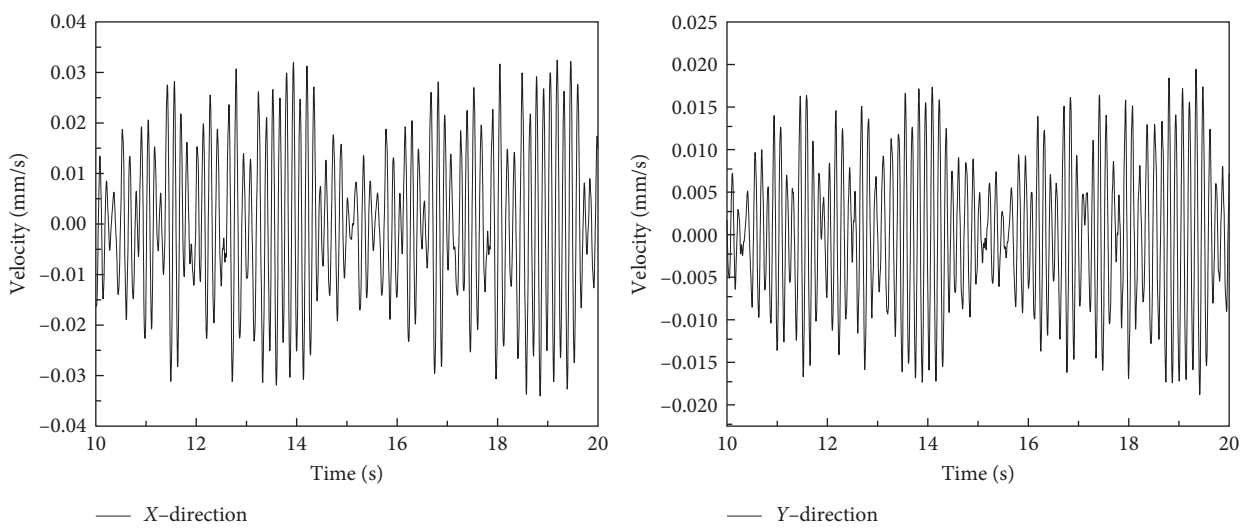

Figure 16: Prediction results of point 6 at each driving velocity in case 2: (a) driving velocity: 8 mm/min; (b) driving velocity: 4 mm/min; and (c) driving velocity: 2 mm/min.

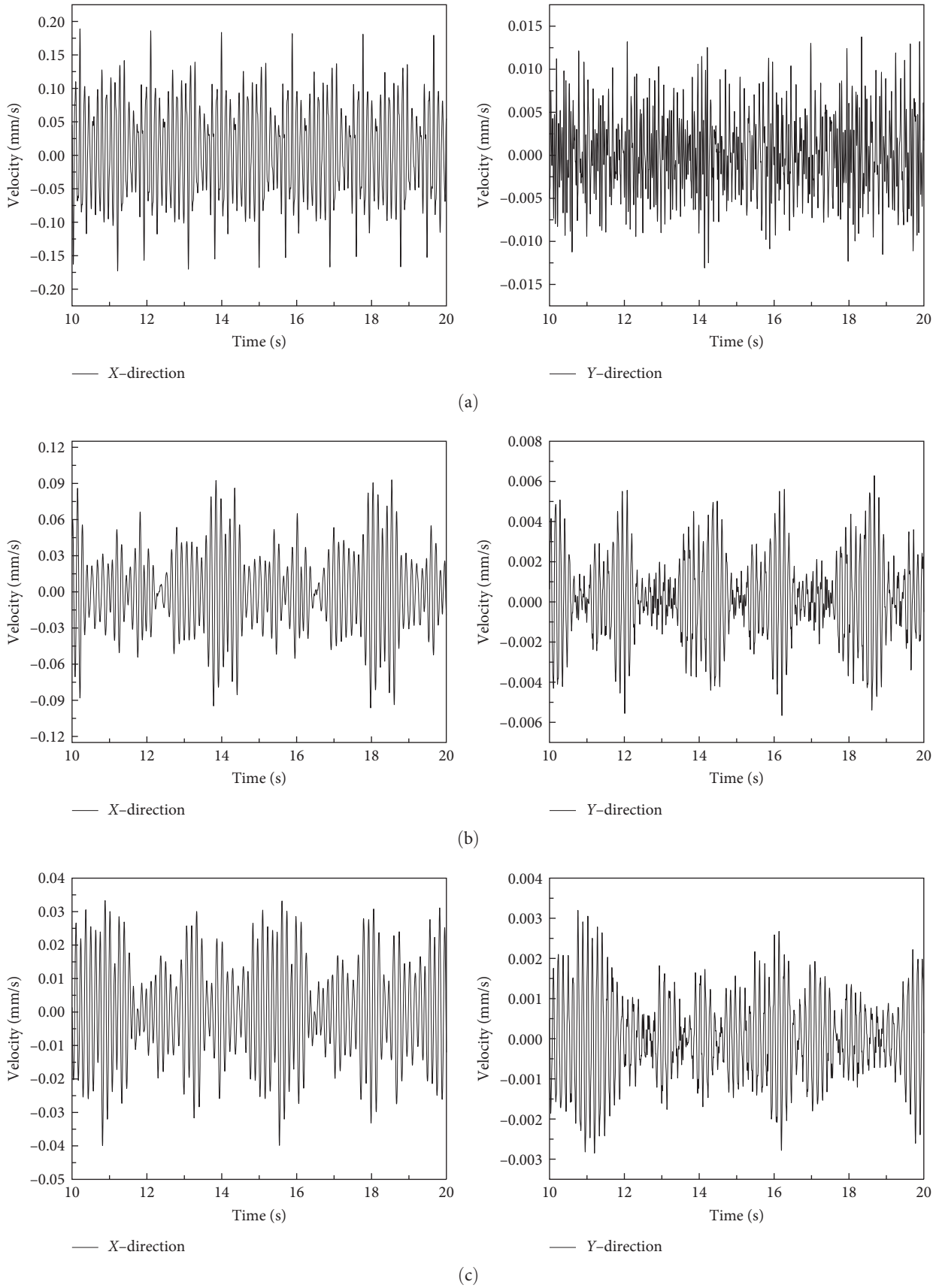

Figure 17: Prediction results of point 6 under each driving velocity in case 3: (a) driving velocity: 8 mm/min; (b) driving velocity: 4 mm/min; and (c) driving velocity: 2 mm/min.

Table 3: Vibration response of case 2 and case 3 under different construction parameters.

Driving velocity (mm/min)	Peak value of X-direction vibration velocity at point 6 (mm/s)	
	Case 2	Case 3
8	0.123	0.183
4	0.065	0.093
2	0.034	0.039

After verifying the feasibility of the model, it is believed that the model has a certain level of accuracy when predicting the vibration of the south line tunnel; the soil layer is excavated on the south side of the north line tunnel to simulate its vibration. The center of the south line tunnel is 34.5 m away from the center of the north line tunnel, and the burial depth is the same as that of the north line tunnel. The input load for simulating the excavation of the south line tunnel under each case is the same as that for the excavation of the north line tunnel under each case, and prediction analysis is carried out for measuring point 6 on the north side of the White Tower (Figure 15).

4.2. Construction Parameter Simulation. The south line tunnel has not been constructed yet. To ensure the safety during its construction, the construction parameters of the south line tunnel are simulated, and the possible vibration response of the corresponding construction parameters on the White Tower is predicted. This can provide guidance for the construction of the south line tunnel. To ensure compliance with safety regulations, a low tunneling velocity is selected. As shown in Figure 16, at a tunneling velocity of 8 mm/min, the simulation results indicate that the peak vibration velocity at measuring point 6 is 0.123 mm/s in the X-direction and 0.0691 mm/s in the Y-direction. The driving velocity is then reduced to 4 mm/min, resulting in a peak vibration velocity of 0.065 mm/s in the X-direction and 0.04 mm/s in the Y-direction at measuring point 6. Considering the more stringent vibration limits for ancient buildings, further simulations are conducted at a driving velocity of 2 mm/min.

At this lower driving velocity, the peak vibration velocity at measuring point 6 is 0.036 mm/s in the X-direction and 0.130 mm/s in the Y-direction. It is important to note that the vibration response in the X-direction is significantly reduced at a driving velocity of 2 mm/min; although, it still exceeds the vibration limit.

In case 3, the shield cutter head is positioned on the same horizontal plane as the White Tower, with a minimum horizontal distance of 24 m between the sideline and the tower. Considering the potential significant influence of shield tunneling vibration on the White Tower in this case, simulations were conducted at different tunneling velocities.

As shown in Figure 17, at a tunneling velocity of 8 mm/min, the simulation results indicate that the peak vibration velocity at measuring point 6 is 0.183 mm/s in the X-direction and 0.0142 mm/s in the Y-direction. Decreasing the driving velocity to 4 mm/min yields a peak vibration velocity of 0.093 mm/s in the X-direction and 0.0063 mm/s in the Y-direction at measuring point 6. Further, reducing the driving velocity to 2 mm/min results in a peak vibration velocity of 0.046 mm/s in the X-direction and 0.003 mm/s in the Y-direction at measuring point 6.

The simulation results for two cases are shown in Table 3. It can be seen that the driving velocity has a significant influence on the vibration response. When the driving velocity is adjusted from 8 to 4 mm/min, the vibration response in the X-direction is reduced by 50% and in the Y-direction by 56%.

5. Conclusion

In this research, taking the White Tower in Hangzhou as an example, the vibration response propagation of ultra-large-diameter shield tunnel excavation to adjacent ancient towers is studied through field measurements. The vibration response of the unexcavated south line tunnel is predicted using 3D numerical analysis software. The following conclusions were drawn based on the research findings:

(1) The vibration magnitude at White Tower bedrock caused by the tunneling of the north line is small, and the vibration level in the parallel shield direction (Y) is greater than that in the transverse direction (X);

(2) The vibration bands inside the rock layer remains stable, which presents a steady-state vibration behavior. When the lateral distance between the source and the receiver on the surface is larger than 40 m, the vibration attenuation is significant;

(3) The vibration response at the White Tower bedrock is correlated with construction parameters (thrust, torque, and driving velocity), and decreasing above construction parameters can reduce the vibration level, particularly the driving velocity. When the driving velocity is reduced from 8 to 2 mm/min, the vibration response can be reduced by up to 72% in the X-direction and up to 78% in the Y-direction.

Data Availability

All data, models, and code generated or used during the study appear in the published article.

Conflicts of Interest

The authors declare that they have no known competing financial interests or personal relationships that could have appeared to influence the work reported in this paper.

Acknowledgments

This work was supported by the National Natural Science Foundation of China (Grant nos. 52078462 and 52378376), Fundamental Research Funds for the Provincial Universities of Zhejiang (no. RF-B2023007), and Zhejiang Province Construction Research Projects (no. 2023K155).

References

[1] P. Fiala, G. Degrande, and F. Augusztinovicz, "Numerical modelling of ground-borne noise and vibration in buildings due to surface rail traffic," *Journal of Sound and Vibration*, vol. 301, no. 3–5, pp. 718–738, 2007.

[2] O. Avci, A. Bhargava, N. Nikitas, and D. J. Inman, "Vibration annoyance assessment of train induced excitations from tunnels embedded in rock," *Science of The Total Environment*, vol. 711, Article ID 134528, 2020.

[3] K. A. Kuo, H. E. M. Hunt, and M. F. M. Hussein, "The effect of a twin tunnel on the propagation of ground-borne vibration from an underground railway," *Journal of Sound and Vibration*, vol. 330, no. 25, pp. 6203–6222, 2011.

[4] L. Wan, X. Xie, L. Wang, P. Li, and Q. Huang, "Modal analysis of subway tunnel in soft soil during operation," *Underground Space*, vol. 8, pp. 181–195, 2023.

[5] C. Zou, J. A. Moore, M. Sanayei, Z. Tao, and Y. Wang, "Impedance model of train-induced vibration transmission across a transfer structure into an over track building in a metro depot," *Journal of Structural Engineering*, vol. 148, no. 11, Article ID 04022187, 2022.

[6] S. Gupta, Y. Stanus, G. Lombaert, and G. Degrande, "Influence of tunnel and soil parameters on vibrations from underground railways," *Journal of Sound and Vibration*, vol. 327, no. 1-2, pp. 70–91, 2009.

[7] J. Zhang, Q. Yan, M. Sun, B. Li, W. Chen, and H. Chen, "Experimental study on the vibration damping of two parallel shield tunnels connected by an assembled transverse passage," *Tunnelling and Underground Space Technology*, vol. 107, Article ID 103659, 2021.

[8] C. Zou, Y. Wang, P. Wang, and J. Guo, "Measurement of ground and nearby building vibration and noise induced by trains in a metro depot," *Science of the Total Environment*, vol. 536, pp. 761–773, 2015.

[9] B. Noori, R. Arcos, A. Clot, and J. Romeu, "Control of ground-borne underground railway-induced vibration from double-deck tunnel infrastructures by means of dynamic vibration absorbers," *Journal of Sound and Vibration*, vol. 461, Article ID 114914, 2019.

[10] C. Zou, Y. Wang, J. A. Moore, and M. Sanayei, "Train-induced field vibration measurements of ground and over-track buildings," *Science of the Total Environment*, vol. 575, pp. 1339–1351, 2017.

[11] L. He and Z. Tao, "Building vibration measurement and prediction during train operations," *Buildings*, vol. 14, no. 1, Article ID 142, 2024.

[12] F. Chen, R. Duan, X. Zhang, J. Liu, C. Sun, and X. Li, "Analysis on vibration influence of the construction of short-distance pile foundation on existing shield tunnels," *Modern Tunnelling Technology*, vol. 60, no. 1, pp. 140–148, 2023.

[13] W. Shiguang and Z. Songye, "Global vibration intensity assessment based on vibration source localization on construction sites: application to vibratory sheet piling," *Applied Sciences*, vol. 12, no. 4, 2022.

[14] M. K. Rainer, W. Carl, and H.F. Bengt, "Dynamic ground response during vibratory sheet pile driving," *Journal of Geotechnical and Geoenvironmental Engineering*, vol. 147, no. 7, 2021.

[15] Z. Li, Y. Cao, M. Ma, and Q. Xiang, "Prediction of ground-borne vibration from random traffic flow and road roughness: theoretical model and experimental validation," *Engineering Structures*, vol. 285, Article ID 116060, 2023.

[16] X. F. Fang and D. Li, "Field test and analysis for environmental vibration induced by road traffic load," *Structural Engineering, Vibration and Aerospace Engineering*, vol. 482, pp. 183–187, 2014.

[17] K. Wu, Y. Zheng, S. Li, J. Sun, Y. Han, and D. Hao, "Vibration response law of existing buildings affected by subway tunnel boring machine excavation," *Tunnelling and Underground Space Technology*, vol. 120, Article ID 104318, 2022.

[18] A. Rallu, N. Berthoz, S. Charlemagne, and D. Branque, "Vibrations induced by tunnel boring machine in urban areas: in situ measurements and methodology of analysis," *Journal of Rock Mechanics and Geotechnical Engineering*, vol. 15, no. 1, pp. 130–145, 2023.

[19] M. Liu, S. Liao, Y. Yang, Y. Men, J. He, and Y. Huang, "Tunnel boring machine vibration-based deep learning for the ground identification of working faces," *Journal of Rock Mechanics and Geotechnical Engineering*, vol. 13, no. 6, pp. 1340–1357, 2021.

[20] Z. Lu, X. Wang, G. Zhou, L. Feng, and Y. Jiang, "Investigation on vibration influence law of double-shield TBM tunnel construction," *Applied Sciences*, vol. 12, no. 15, Article ID 7727, 2022.